

Partial equilibrium approximations in Apoptosis

Ya-Jing Huang*, Wen-An Yong†

Abstract

Apoptosis is one of the most basic biological processes. In apoptosis, tens of species are involved in many biochemical reactions with times scales of widely differing orders of magnitude. By the law of mass action, the process is mathematically described with a large and stiff system of ODEs (ordinary differential equations). The goal of this work is to simplify such systems of ODEs with the PEA (partial equilibrium approximation) method. In doing so, we propose a general framework of the PEA method together with some conditions, under which the PEA method can be justified rigorously. The main condition is the principle of detailed balance for fast reactions as a whole. With the justified method as a tool, we made many attempts via numerical tests to simplify the Fas-signaling pathway model due to Hua et al. (2005) and found that nine of reactions therein can be well regarded as relatively fast. This paper reports our simplification of Hua et al.'s model with the PEA method based on the fastness of the nine reactions, together with numerical results which confirm the reliability of our simplified model.

Keywords: Partial equilibrium approximation, apoptosis, biochemical reactions, the principle of detailed balance, sensitivity analysis

1 Introduction

Apoptosis is one of the most basic biological phenomena. It is a cellular suicide route that allows for the selective removal of superfluous and potentially dangerous cells. This genetically controlled process ensures normal embryonic development, tissue homeostasis and normal immune-system function in multicellular organisms. On the other hand, defects in apoptosis may cause serious diseases such as cancer, autoimmunity, and neurodegeneration [1, 2, 3, 4]. For these reasons, understanding the mechanism of apoptosis is of fundamental importance.

The apoptotic process involves tens of biological molecules (species), which react within tens of biochemical reactions with time scales of widely differing orders of magnitude. When the law of mass action [5] is employed, it is described mathematically by a simultaneous system of tens of ordinary differential equations (ODEs). Such a large scale and stiff system of ODEs can hardly help us to understand the mechanism of the apoptosis.

*Zhou Pei-Yuan Center for Appl. Math., Tsinghua university, Beijing 100084, China; Email: huangyj09@mails.tsinghua.edu.cn

†Zhou Pei-Yuan Center for Appl. Math., Tsinghua university, Beijing 100084, China; Email: wayong@tsinghua.edu.cn

The goal of this work is to derive mathematically reliable simplifications of the large apoptosis system proposed by Hua et al. in [6] for human Jurkat T cells. Two widely used methods for simplifying chemical kinetics are the Quasi Steady-State Approximation (QSSA) [7, 8], also called the Bodenstein method, and Partial Equilibrium Approximation (PEA) [9, 10, 11]. The former assumes that the concentrations of transient intermediate species reach steady states and thereby the rate equations for the intermediate species are replaced with algebraic relations. On the other hand, the PEA simply takes the fast reactions in equilibrium. In this manner, the stiffness is removed and some algebraic constraints are obtained. For both methods, the algebraic relations can be used to reduce the number of the rate equations and consequently the chemical kinetics is simplified. An unexpected benefit of such simplifications is that less parameters are needed for the simplified models than for the original ones. This is good because the parameters are often not reliably known (see [9]).

The QSSA, PEA and their combinations have been extensively used to simplify chemical kinetics mechanisms for many years, with great success [12, 13, 14, 15, 16, 17, 18]. They were also used by Okazaki et al. in [19] to simplify the large apoptosis system in [6] (see comments below). However, these methods seem to lack a systematically mathematical justification. Recently, we pointed out that the PEA method can be rigorously justified for reversible reactions obeying the principle of detailed balance [20, 21], by using the singular perturbation theory of initial-value problems for ODEs [22]. Thus, our simplification will base on this justified PEA method and therefore is reliable.

As commented in [23], Okazaki et al.'s simplification seems baseless. In fact, when applying the QSSA method for the intermediate species Casp8^{*}-Casp3, Okazaki et al. assumed that the concentration sum of the intermediate species and Casp8^{*} (an activated initiator caspase) was conserved and obtained the Michaelis-Menten equation for the product (see Appendix A of [19]). The latter is only true if the activated initiator caspase does not participate in other reactions. However, this is not the case here because the activated caspase is simultaneously, instead of consecutively, involved in other reactions. Similar conservation assumptions were used for several steps. This is why we question the simplified model in [19], although it is successful in some sense.

This paper is a continuation of our previous work [23]. In [23], we showed that two molecules (Smac and XIAP) involved in the apoptotic process, neglected in [19], are not negligible in general. Then we applied the justified PEA method to obtain a very preliminary simplified model by assuming only six reversible reactions to be fast. In the present paper, we will use the PEA method to further simplify the large apoptosis system [6]. To do this, we firstly verify the principle of detailed balance for more fast reactions as a whole. Having such a verification, the singular perturbation theory of initial-value problems for ODEs can be employed to derive our simplified models. Then we use numerical simulations to compare the new models with the original one and Okazaki et al.'s simplified model from various aspects, including accuracy, sensitivity and the M-D transition behavior [19]. Moreover, we introduce a new quantity to evaluate our simplifications. All numerical results confirm the reliability of both our simplified models and the PEA method.

Let us remark that, thanks to its reliability, the justified PEA could be used as a tool to determine whether or not a reversible reaction is relatively fast. To this end, one could numerically compare the

solution of partial equilibrium computation with that of the fully non-equilibrium computation. If the two solutions are close to each other, the reaction can be claimed to be relatively fast.

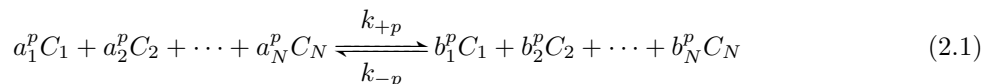
The paper is organized as follows. In Section 2 we present a general framework of the PEA method, together with some conditions under which the method can be justified rigorously. The apoptosis process is introduced in Section 3. The PEA method is used in Section 4 to simplify the apoptosis system by checking the principle of detailed balance for nine reversible reactions as a whole. Numerical simulations are reported in Section 5. Finally, the main results of this paper are summarized in Section 5.

2 The PEA Method

In this section we first present a general framework of the PEA method, together with some conditions under which the method can be justified rigorously. Then we take the simplest system for enzyme inhibition as an example to show how to use our PEA method.

2.1 A general framework of the PEA method

Consider a system with N chemical species $C_i (i = 1, 2, \dots, N)$ participating in M reactions



for $p = 1, 2, \dots, M$. Here the non-negative integers a_i^p and b_i^p are the stoichiometric coefficients of the i^{th} -species in the p^{th} -reaction, and k_{+p} and k_{-p} are the respective forward and backward rate constants of the p^{th} -reaction. The reversibility means that both k_{+p} and k_{-p} are positive.

Denote by $u_i = [C_i](t)$ the concentration of the i^{th} -species C_i at time t . According to the law of mass action [5], the evolution equation for u_i is

$$\frac{du_i}{dt} = \sum_{p=1}^M (b_i^p - a_i^p) v_p \quad (2.2)$$

with

$$v_p = k_{+p} u_1^{a_1^p} u_2^{a_2^p} \dots u_N^{a_N^p} - k_{-p} u_1^{b_1^p} u_2^{b_2^p} \dots u_N^{b_N^p}$$

being the reaction rate of the p -th reaction.

Suppose the first $M' (\leq M)$ reactions in (2.1) are much faster than others. Then the kinetic equations in (2.2) can be rewritten in the vectorial form:

$$\begin{aligned} \frac{dV}{dt} &= \frac{1}{\varepsilon} Q_1(V) + Q_2(V, Z), \\ \frac{dZ}{dt} &= Q_3(V, Z). \end{aligned} \quad (2.3)$$

Here V is an N' -vector consisting of those u_i so that the i^{th} -species participates in the fast reactions, Z consists of the rest u_i , ε is a small positive parameter characterizing the fastness, and $Q_1(V), Q_2(V, Z)$

and $Q_3(V, Z)$ stand for the corresponding reaction rates. The introduction of ε is to make $Q_1(V)$ have the same order of magnitude as $Q_2(V, Z)$ and $Q_3(V, Z)$. A special case is that Z is void and V contains all u_i .

Assume that there is a steady state $u^* = (u_1^*, u_2^*, \dots, u_N^*)$ satisfying $u_i^* > 0$ for all i and a zero net flux condition for each fast reaction:

$$k_{+p}(u_1^*)^{a_1^p}(u_2^*)^{a_2^p} \dots (u_N^*)^{a_N^p} - k_{-p}(u_1^*)^{b_1^p}(u_2^*)^{b_2^p} \dots (u_N^*)^{b_N^p} = 0, \quad \forall p = 1, 2, \dots, M'.$$

This is just the principle of detailed balance [20] for the partial system consisting of the fast reactions merely. Clearly, it can only be true when both k_{+p} and k_{-p} are positive, that is, reversible reactions.

Under this assumption, we know from [21] that there is a strictly convex function $\eta = \eta(V)$ so that $Q_1(V)$ can be written as

$$Q_1(V) = S(V)\eta_V(V)$$

for V with strictly positive components. Here $S(V)$ is a symmetric matrix with null-space independent of V and $\eta_V(V)$ is the gradient of $\eta(V)$. Moreover, the singular perturbation theory [22] for initial-value problems of ODEs can be applied to the stiff system in (2.3). In particular, the solutions to initial-value problems of (2.3) converge uniformly to those of a corresponding reduced system, as ε goes to zero, in any bounded time interval away from zero.

In order to derive the reduced system, we notice the V -independence of the null-space and denote by Π the constant matrix whose rows span the left null-space of $S(V)$. Without loss of generality, we assume that Π is of the form

$$\Pi = (\Theta, I)$$

with I the unit matrix of proper order. Accordingly, we introduce the partition

$$V = \begin{pmatrix} X \\ Y \end{pmatrix}, \quad Q_1(V) = \begin{pmatrix} \hat{Q}_1(X, Y) \\ \hat{Q}_2(X, Y) \end{pmatrix}, \quad Q_2(V, Z) = \begin{pmatrix} \tilde{Q}_1(X, Y, Z) \\ \tilde{Q}_2(X, Y, Z) \end{pmatrix}.$$

This partition ensures that X can be uniquely and globally obtained by solving $\hat{Q}_1(X, \tilde{Y} - \Theta X) = 0$ (see [21] if necessary).

Define

$$\tilde{Y} = Y + \Theta X.$$

The kinetic equations in (2.3) can be rewritten as

$$\begin{aligned} \frac{dX}{dt} &= \frac{1}{\varepsilon} \hat{Q}_1(X, \tilde{Y} - \Theta X) + \tilde{Q}_1(X, \tilde{Y} - \Theta X, Z), \\ \frac{d\tilde{Y}}{dt} &= \tilde{Q}_2(X, \tilde{Y} - \Theta X, Z) + \Theta \tilde{Q}_1(X, \tilde{Y} - \Theta X, Z), \\ \frac{dZ}{dt} &= Q_3(X, \tilde{Y} - \Theta X, Z). \end{aligned} \tag{2.4}$$

As ε goes to zero, the reduced system for (2.4) is

$$\begin{aligned}\hat{Q}_1(X, \tilde{Y} - \Theta X) &= 0, \\ \frac{d\tilde{Y}}{dt} &= \tilde{Q}_2(X, \tilde{Y} - \Theta X, Z) + \Theta \tilde{Q}_1(X, \tilde{Y} - \Theta X, Z), \\ \frac{dZ}{dt} &= Q_3(X, \tilde{Y} - \Theta X, Z).\end{aligned}\tag{2.5}$$

From $\hat{Q}_1(X, \tilde{Y} - \Theta X) = 0$ we solve X in terms of \tilde{Y} , say $X = \Phi(\tilde{Y})$. Substituting this expression into the second and third equations in (2.5), we obtain

$$\begin{cases} \frac{d\tilde{Y}}{dt} = \tilde{Q}_2(\Phi(\tilde{Y}), \tilde{Y} - \Theta\Phi(\tilde{Y}), Z) + \Theta\tilde{Q}_1(\Phi(\tilde{Y}), \tilde{Y} - \Theta\Phi(\tilde{Y}), Z), \\ \frac{dZ}{dt} = Q_3(\Phi(\tilde{Y}), \tilde{Y} - \Theta\Phi(\tilde{Y}), Z). \end{cases}$$

This is our simplified model by using the PEA method. Note that the original variables X and Y are recovered from

$$X = \Phi(\tilde{Y}), \quad Y = \tilde{Y} - \Theta\Phi(\tilde{Y}).$$

In case X can be solved from $\hat{Q}_1(X, Y) = 0$ in terms of Y , say $X = \Psi(Y)$, we recall the fact that X can be obtained by solving $\hat{Q}_1(X, \tilde{Y} - \Theta X) = 0$ and may well assume that both the Jacobian matrices \hat{Q}_{1X} (of $\hat{Q}_1(X, Y)$ with respect to X) and $[\hat{Q}_{1X} - \hat{Q}_{1Y}\Theta]$ are invertible. Then $[I - \hat{Q}_{1X}^{-1}\hat{Q}_{1Y}\Theta] = \hat{Q}_{1X}^{-1}[\hat{Q}_{1X} - \hat{Q}_{1Y}\Theta]$ is invertible. It is an easy exercise to show that the invertibility of $[I - \hat{Q}_{1X}^{-1}\hat{Q}_{1Y}\Theta]$ is equivalent to that of $[I - \Theta\hat{Q}_{1X}^{-1}\hat{Q}_{1Y}]$. On the other hand, we deduce from $\hat{Q}_1(\Psi(Y), Y) = 0$ that $\hat{Q}_{1X}\Psi(Y)_Y + \hat{Q}_{1Y} = 0$ and thereby $\Psi(Y)_Y = -\hat{Q}_{1X}^{-1}\hat{Q}_{1Y}$. Now we compute from $\tilde{Y} = Y + \Theta\Psi(Y)$ that

$$\frac{d\tilde{Y}}{dt} = \frac{dY}{dt} + \Theta\Psi(Y)_Y \frac{dY}{dt} = [I - \Theta\hat{Q}_{1X}^{-1}\hat{Q}_{1Y}] \frac{dY}{dt}.$$

Thus we gain equations for Y :

$$\frac{dY}{dt} = (I + \Theta\Psi(Y)_Y)^{-1}(\tilde{Q}_2(\Psi(Y), Y, Z) + \Theta\tilde{Q}_1(\Psi(Y), Y, Z)).$$

Consequently, the reduced system can be written as

$$\begin{aligned}\frac{dY}{dt} &= (I + \Theta\Psi(Y)_Y)^{-1}(\tilde{Q}_2(\Psi(Y), Y, Z) + \Theta\tilde{Q}_1(\Psi(Y), Y, Z)), \\ \frac{dZ}{dt} &= Q_3(\Psi(Y), Y, Z)\end{aligned}\tag{2.6}$$

together with the algebraic relation $X = \Psi(Y)$.

2.2 A simple example

In order to elucidate how to use the PEA method, we consider the simplest system for enzyme inhibition [5]. This system is demonstrated graphically in Fig. 1 and reveals the competitively inhibitory mechanism, where the enzyme reaction is stopped when the inhibitor is bound to the active site of the enzyme. In

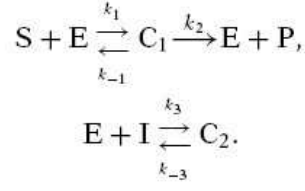


Figure 1: The simplest mechanism for enzyme inhibition

Fig. 1, the symbols E, S, I, P, C_1 and C_2 stand for the enzyme, the substrate, the inhibitor, the product and two complexes, respectively. k_1 and k_{-1} are the respective kinetic rate constants of the forward and backward reaction for substrate binding, while k_3 and k_{-3} are those of the inhibitor binding reaction. k_2 is the rate constant of the substrate conversion reaction.

According to law of mass action, the corresponding kinetic equations read as

$$\begin{aligned}
\frac{d[C_1]}{dt} &= v_1 - v_2 \\
\frac{d[C_2]}{dt} &= v_3 \\
\frac{d[E]}{dt} &= -v_1 - v_3 + v_2 \\
\frac{d[S]}{dt} &= -v_1 \\
\frac{d[I]}{dt} &= -v_3 \\
\frac{d[P]}{dt} &= v_2.
\end{aligned} \tag{2.7}$$

with

$$\begin{aligned}
v_1 &= k_1[E][S] - k_{-1}[C_1], \\
v_2 &= k_2[C_1], \\
v_3 &= k_3[E][I] - k_{-3}[C_2].
\end{aligned}$$

Classically, the reactions for enzyme to bind to substrates and inhibitors are regarded as fast and reversible. Thus we rewrite (2.7) as

$$\begin{aligned}
\frac{d[C_1]}{dt} &= \frac{1}{\varepsilon} \hat{v}_1 - v_2 \\
\frac{d[C_2]}{dt} &= \frac{1}{\varepsilon} \hat{v}_3 \\
\frac{d[E]}{dt} &= -\frac{1}{\varepsilon} \hat{v}_1 - \frac{1}{\varepsilon} \hat{v}_3 + v_2 \\
\frac{d[S]}{dt} &= -\frac{1}{\varepsilon} \hat{v}_1 \\
\frac{d[I]}{dt} &= -\frac{1}{\varepsilon} \hat{v}_3 \\
\frac{d[P]}{dt} &= v_2.
\end{aligned} \tag{2.8}$$

where $\hat{v}_1 = \varepsilon v_1$, $\hat{v}_3 = \varepsilon v_3$, and \hat{v}_1 and \hat{v}_3 have the same order of magnitude as v_2 . Thanks to the reversibility, it is obvious that there are positive numbers $[E]^*$, $[S]^*$, $[C_1]^*$, $[I]^*$ and $[C_2]^*$ such that

$$v_1 = k_1[E]^*[S]^* - k_{-1}[C_1]^* = 0, \quad v_3 = k_3[E]^*[I]^* - k_{-3}[C_2]^* = 0.$$

Thus the PEA method above can be well applied to the stiff system (2.8).

The reduced system for (2.8) can be derived as follows. Set

$$\begin{aligned} X &= ([C_1], [C_2])^T, \\ Y &= ([E], [S], [I])^T, \\ Z &= [P]. \end{aligned}$$

the stiff system (2.8) can be rewritten as

$$\begin{aligned} \frac{dX}{dt} &= \frac{1}{\varepsilon} \begin{pmatrix} \hat{v}_1 \\ \hat{v}_3 \end{pmatrix} + v_2 \begin{pmatrix} -1 \\ 0 \end{pmatrix}, \\ \frac{d(Y + \Theta X)}{dt} &= v_2 \begin{pmatrix} 0 \\ -1 \\ 0 \end{pmatrix}, \\ \frac{d[P]}{dt} &= v_2 \end{aligned} \tag{2.9}$$

with

$$\Theta = \begin{pmatrix} 1 & 1 \\ 1 & 0 \\ 0 & 1 \end{pmatrix}.$$

From $\hat{v}_1 = \hat{v}_3 = 0$, we get

$$[C_1] = K_1[E][S], \quad [C_2] = K_3[E][I] \tag{2.10}$$

with $K_j = k_j/k_{-j}$ for $j = 1, 3$. Substituting these into the last two equations in (2.9), we obtain the following ODEs

$$\begin{aligned} \frac{d([E] + [C_1] + [C_2])}{dt} &= 0, \\ \frac{d([S] + [C_1])}{dt} &= -k_2 K_1 [E][S], \\ \frac{d([I] + [C_2])}{dt} &= 0, \\ \frac{d[P]}{dt} &= k_2 K_1 [E][S]. \end{aligned}$$

This, together with (2.10), is the simplified model by using the justified PEA method. This model can be further simplified by using the conservation laws indicated in the first and third equations. We omit it here and leave it to the interested reader.

3 Apoptosis Systems

Here we introduce the large apoptosis system proposed by Hua et al. in [6] for human Jurkat T cells. To begin with, we recall that there are at least two pathways to trigger apoptosis—intrinsic (mitochondrial) and extrinsic (death receptor) signalling pathways. Both induce death-associated proteolytic and/or nucleolytic activities. The intrinsic pathway is initiated when the cell is severely damaged or stressed, while the extrinsic one is activated when extracellular death ligands are bound by their cognate membrane-associated death receptors such as TNF-R1(DR1,p55), Fas(DR2,CD95), DR3(APO-3,TRAMP), DR4(APO-2,TRAIL-R1) and DR5(TRICK2,TRAOL-R2) [1, 24, 25, 26, 27].

The Fas-induced signaling pathway is among the best understood and can be schematically shown in Fig. 2. It begins with the binding of Fas ligands (FasL), Fas and FADD (Fas-associated death domain) to form the complex DISC (death-inducing signaling complex). The latter can recruit initiator caspases such as caspase-8 (Casp8) molecules to cleave and activate them. The activated initiator caspase (Casp8₂^{*}) can cleave and activate the executor caspase-3 (Casp3) to form Casp3^{*} directly. The amount of Casp3^{*} is the indicator of apoptosis. This way to activate Casp3 is called D-channel. In addition, Casp3 can also be activated in a so-called M-channel. In this channel, Casp8₂^{*} cleaves Bid to generate truncated (t)Bid. The tBid then binds to two molecules of Bax to form a complex tBid:Bax₂, which will induce the release of Cyto.c and Smac from the mitochondria. The released Cyto.c^{*} will combine an adaptor protein Apaf-1, ATP and caspase-9 to form apoptosome and thereby activate caspase-9. The activated caspase-9 (Casp9^{*}) cleaves and activates Casp3. On the other hand, the M-channel can be blocked by XIAP (X-linked inhibitor of apoptosis protein) and Bcl2 through their bindings to the released Smac^{*}, Casp9, Casp3^{*}, Bax and tBid.

The Fas-signaling pathway model proposed by Hua et al. [6] consists of biochemical reactions (H1)–(H25) given in Table 1. From this table we see that the process activating the initiator caspase-8 (Casp8) consists of the reactions from (H1) to (H6), which is initiated by FasL. The activated Casp8₂^{*} enzymatically cleaves caspase-3(Casp3) to produce activated executor Casp3^{*} ((H7) and (H8)) and Bid to generate tBid ((H9) and (H10)) simultaneously. Then the tBid associates with two Bax to form tBid:Bax₂ through (H11) and (H12), which induces the release of Cyto.c and Smac from mitochondrial to cytosol ((H15) and (H13)). The released Cyto.c (Cyto.c^{*}) combines Apaf (Apaf-1) and ATP to form an apoptosome (Cyto.c^{*}:Apaf:ATP) in (H16), which recruits two caspase-9(Casp9) and generates the activated caspase-9 (Casp9^{*}) through (H17) to (H19). The activated Casp9^{*} can also enzymatically cleave and activate caspase-3 ((H20) and (H21)). On the other hand, the roles of Casp9, Casp3^{*}, tBid and Bax can be inhibited by binding to XIAP((H22) and (H23)) and Bcl₂ ((H24) and (H25)), while the released Smac (Smac^{*}) can suppress the function of XIAP (H14). Table 1 also contains all the forward/backward rate constants $k_{\pm i}$ ($i = 1, 2, \dots, 25$).

Observe that not every reaction in Table 1 is reversible and the reactions activating Casp8 are independent of the rest. As in [19], we call the downstream process, consisting of reactions from (H7) to (H25), as the intracellular-signaling subsystem (ISS). Moreover, we follow [19] and assume that the concentration of ATP is a fixed constant. Thus, there are 28 species and 19 biochemical reactions involved

Table 1: The Fas-signaling pathway model due to Hua et al. (2005)

Reaction		k_i	k_{-i}
(H1)	$FasL + Fas \xrightleftharpoons[k_{-H1}]{k_{H1}} FasC$	$9.09 \times 10^{-5} n M^{-1} s^{-1}$	1.00×10^{-4}
(H2) ^a	$FasC : FADD_p : Casp8_q : FLIP_r + FADD \xrightleftharpoons[k_{-H2}]{k_{H2}} Fas : FADD_{p+1} : Casp8_q : FILP_r$	$5.00 \times 10^{-4} n M^{-1} s^{-1}$	0.2
(H3) ^b	$FasC : FADD_p : Casp8_q : FILP_r + Casp8 \xrightleftharpoons[k_{-H3}]{k_{H3}} Fas : FADD_p : Casp8_{q+1} : FILP_r$	$3.50 \times 10^{-3} n M^{-1} s^{-1}$	0.018
(H4) ^b	$FasC : FADD_p : Casp8_q : FLIP_r + FILP \xrightleftharpoons[k_{-H4}]{k_{H4}} Fas : FADD_p : Casp8_q : FILP_{r+1}$	$3.50 \times 10^{-3} n M^{-1} s^{-1}$	0.018
(H5) ^c	$FasC : FADD_p : Casp8_q : FLIP_r \xrightarrow{k_{H5}} Casp8_{*2} : p41 + FasC : FADD_p : Casp8_{q-1} : FILP_r$	$0.3 s^{-1}$	
(H6)	$Casp8_{*2} : p41 \xrightarrow{k_{H6}} Casp8_{*2}$	$0.1 s^{-1}$	
(H7)	$Casp8_{*2} + Casp3 \xrightleftharpoons[k_{-H7}]{k_{H7}} Casp8_{*2} : Casp3$	$1.00 \times 10^{-4} n M^{-1} s^{-1}$	0.06
(H8)	$Casp8_{*2} : Casp3 \xrightarrow{k_{H8}} Casp8_{*2} + Casp3^*$	$0.1 s^{-1}$	
(H9)	$Casp8_{*2} + Bid \xrightleftharpoons[k_{-H9}]{k_{H9}} Casp8_{*2} : Bid$	$5.00 \times 10^{-4} n M^{-1} s^{-1}$	0.005
(H10)	$Casp8_{*2} : Bid \xrightarrow{k_{H10}} Casp8_{*2} + tBid$	$0.1 s^{-1}$	
(H11)	$tBid + Bax \xrightleftharpoons[k_{-H11}]{k_{H11}} tBid : Bax$	$2.00 \times 10^{-4} n M^{-1} s^{-1}$	0.02
(H12)	$tBid : Bax + Bax \xrightleftharpoons[k_{-H12}]{k_{H12}} tBid : Bax_2$	$2.00 \times 10^{-4} n M^{-1} s^{-1}$	0.02
(H13)	$Smac + tBid : Bax_2 \xrightarrow{k_{H13}} Smac^* + tBid : Bax_2$	$1.00 \times 10^{-3} n M^{-1} s^{-1}$	
(H14)	$Smac^* + XIAP \xrightleftharpoons[k_{-H14}]{k_{H14}} Smac^* : XIAP$	$7.00 \times 10^{-3} n M^{-1} s^{-1}$	2.21×10^{-3}
(H15)	$Cyto.c + tBid : Bax_2 \xrightarrow{k_{H15}} Cyto.c^* + tBid : Bax_2$	$1.00 \times 10^{-3} n M^{-1} s^{-1}$	
(H16)	$Cyto.c^* + Apaf + ATP \xrightleftharpoons[k_{-H16}]{k_{H16}} Cyto.c^* : Apaf : ATP$	$2.78 \times 10^{-7} n M^{-1} s^{-1}$	5.70×10^{-3}
(H17)	$Cyto.c^* : Apaf : ATP + Casp9 \xrightleftharpoons[k_{-H17}]{k_{H17}} Cyto.c^* : Apaf : ATP : Casp9$	$2.84 \times 10^{-4} n M^{-1} s^{-1}$	0.07493
(H18)	$Cyto.c^* : Apaf : ATP : Casp9 + Casp9 \xrightleftharpoons[k_{-H18}]{k_{H18}} Cyto.c^* : Apaf : ATP : Casp9_2$	$4.41 \times 10^{-4} n M^{-1} s^{-1}$	0.1
(H19)	$Cyto.c^* : Apaf : ATP : Casp9_2 \xrightarrow{k_{H19}} Cyto.c^* : Apaf : ATP : Casp9 + Casp9^*$	$0.7 s^{-1}$	
(H20)	$Casp9^* + Casp3 \xrightleftharpoons[k_{-H20}]{k_{H20}} Casp9^* : Casp3$	$1.96 \times 10^{-5} n M^{-1} s^{-1}$	0.05707
(H21)	$Casp9^* : Casp3 \xrightarrow{k_{H21}} Casp9^* + Casp3^*$	$4.8 s^{-1}$	
(H22)	$Casp9 + XIAP \xrightleftharpoons[k_{-H22}]{k_{H22}} Casp9 : XIAP$	$1.06 \times 10^{-4} n M^{-1} s^{-1}$	1.00×10^{-3}
(H23)	$Casp3^* + XIAP \xrightleftharpoons[k_{-H22}]{k_{H22}} Casp3^* : XIAP$	$2.47 \times 10^{-3} n M^{-1} s^{-1}$	2.40×10^{-3}
(H24)	$Bcl_2 + Bax \xrightleftharpoons[k_{-H24}]{k_{H24}} Bcl_2 : Bax$	$2.00 \times 10^{-4} n M^{-1} s^{-1}$	0.02
(H25)	$Bcl_2 + tBid \xrightleftharpoons[k_{-H25}]{k_{H25}} Bcl_2 : tBid$	$2.00 \times 10^{-4} n M^{-1} s^{-1}$	0.02

The index (p, q, r) in reactions (a) takes values $(0,0,0), (1,0,0), (1,0,1), (1,1,0), (2,0,0), (2,0,1), (2,0,2), (2,1,0), (2,1,1)$ and $(2,2,0)$. In reactions (b) it takes values $(1,0,0), (2,0,0), (2,0,1), (2,1,0), (3,0,0), (3,0,1), (3,0,2), (3,1,0), (3,1,1)$ and $(3,2,0)$, while it takes values $(2,2,0), (3,2,0), (3,2,1)$ and $(3,3,0)$ in reactions (c).

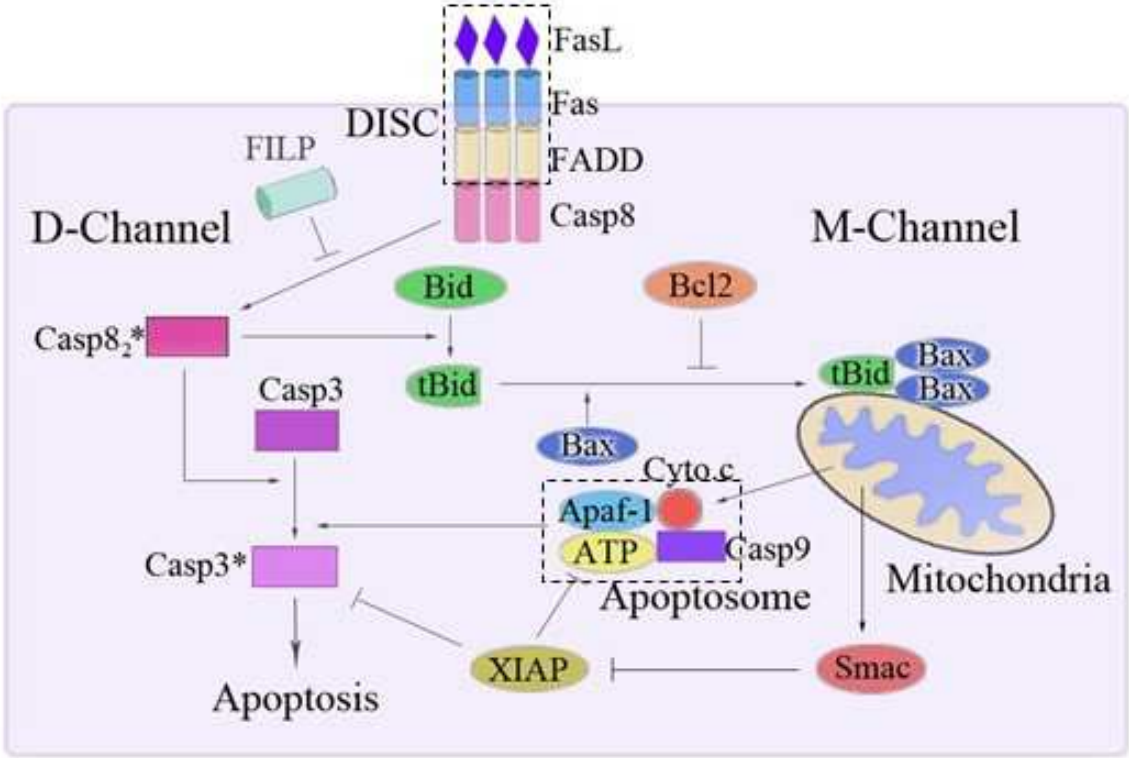


Figure 2: The Fas-induced apoptotic pathway, including two channels.

in the downstream process.

According to the law of mass action, the dynamics of the ISS is governed by 28 ordinary differential equations

$$\frac{dU}{dt} = Q(U). \quad (3.1)$$

Here $U = U(t)$ is a column vector with 28 components representing the concentrations of all the 28 species in the ISS:

$$U = \left([Casp8_2^*], [Casp8_2^* : Casp3], [Casp8_2^* : Bid], [Bid], [tBid], [tBid : Bax], [tBid : Bax_2], [Bcl_2 : tBid], [Bax], [Bcl_2 : Bax], [Bcl_2], [Cyto.c], [Cyto.c^*], [Cyto.c^* : Apaf : ATP], [Cyto.c^* : Apaf : ATP : Casp9], [Cyto.c^* : Apaf : ATP : Casp9_2], [Apaf], [Casp9^*], [Casp9], [Casp3], [Casp9^* : Casp3], [Casp3^*], [Smac], [Smac^*], [XIAP], [Smac^* : XIAP], [Casp9 : XIAP], [Casp3^* : XIAP] \right)^T,$$

each element of the vector-valued function $Q(U)$ of U is the change rate of concentration for the corresponding species

$$Q(U) = \left(-v_7 + v_8 - v_9 + v_{10} + v_0, v_7 - v_8, v_9 - v_{10}, -v_9, v_{10} - v_{11} - v_{25}, v_{11} - v_{12}, v_{12}, v_{25}, -v_{11} - v_{12} - v_{24}, v_{24}, -v_{24} - v_{25}, -v_{15}, v_{15} - v_{16}, v_{16} - v_{17}, v_{17} - v_{18} + v_{19}, v_{18} - v_{19}, -v_{16}, v_{19} - v_{20} + v_{21}, -v_{17} - v_{18} - v_{22}, -v_7 - v_{20}, v_{20} - v_{21}, v_8 + v_{21} - v_{23}, -v_{13}, v_{13} - v_{14}, -v_{14} - v_{22} - v_{23}, v_{14}, v_{22}, v_{23} \right)^T$$

Table 2: Non-zero initial concentrations of the species in the ISS model (Hua. et al. 2005)

Species	Initial concentration(nM)
Casp3	200.00
Bid	25.00
Bcl2	75.00
Bax	83.33
Cyto.c	100.00
Smac	100.00
XIAP	30.00
Casp9	20.00
ATP	10000.00
Apaf	100.00

with $v_i (i = 7 \cdots 25)$ the rate of the i -th reaction in Table 1:

$$\begin{aligned}
v_7 &= k_7[Casp8_2^*][Casp3] - k_{-7}[Casp8_2^* : Casp3], \\
v_8 &= k_8[Casp8_2^* : Casp3], \\
v_9 &= k_9[Casp8_2^*][Bid] - k_{-9}[Casp8_2^* : Bid], \\
v_{10} &= k_{10}[Casp8_2^* : Bid], \\
v_{11} &= k_{11}[tBid][Bax] - k_{-11}[tBid : Bax], \\
v_{12} &= k_{12}[tBid : Bax][Bax] - k_{-12}[tBid : Bax_2], \\
v_{13} &= k_{13}[Smac][tBid : Bax_2] \\
v_{14} &= k_{14}[Smac^*][XIAP] - k_{-14}[Smac^* : XIAP], \\
v_{15} &= k_{15}[Cyto.c][tBid : Bax_2], \\
v_{16} &= k_{16}[Cyto.c^*][Apaf][ATP] - k_{-16}[Cyto.c^* : Apaf : ATP], \\
v_{17} &= k_{17}[Cyto.c^* : Apaf : ATP][Casp9] - k_{-17}[Cyto.c^* : Apaf : ATP : Casp9], \\
v_{18} &= k_{18}[Cyto.c^* : Apaf : ATP : Casp9][Casp9] - k_{-18}[Cyto.c^* : Apaf : ATP : Casp9_2], \\
v_{19} &= k_{19}[Cyto.c^* : Apaf : ATP : Casp9_2], \\
v_{20} &= k_{20}[Casp9^*][Casp3] - k_{-20}[Casp9^* : Casp3], \\
v_{21} &= k_{21}[Casp9^* : Casp3], \\
v_{22} &= k_{22}[Casp9][XIAP] - k_{-22}[Casp9 : XIAP], \\
v_{23} &= k_{23}[Casp3^*][XIAP] - k_{-23}[Casp3^* : XIAP], \\
v_{24} &= k_{24}[Bcl2][Bax] - k_{-24}[Bcl2 : Bax], \\
v_{25} &= k_{25}[Bcl2][tBid] - k_{-25}[Bcl2 : tBid],
\end{aligned}$$

v_0 is the constant rate of generation for Casp8₂^{*} from the upstream process and its value was suggested in [19] as $v_0 = 0.001nMs^{-1}$. In addition, the non-zero initial concentrations for U are taken as in [6, 19] and are given in Table 2.

In [19], Okazaki et al. claimed that Smac and XIAP have little effect on the reaction process of the ISS by studying the M-D transition behavior of both the ISS model and ISS(wo/S,X) (without Smac and XIAP) model. So they did not consider reactions (H13), (H14), (H22) and (H23) in their simplification.

However, in our previous paper [23] we found that Smac and XIAP should not be ignored because the numerical results of these two models are quite different if initial concentrations are changed. Therefore, our sequel discussion will base on the entire ISS system.

We conclude this section by explaining the M-D transition behavior. It means a D-channel and M-channel switching behavior and the quantity of $[Casp8_2^*]$ is a control parameter. When a large amount of $Casp8_2^*$ is activated from the upstream process, it will directly induce cell death through the D-channel; otherwise, the M-channel plays more important role for cell death. In [6], the authors claimed that the effects of D-channel and M-channel can be altered by varying the amount of $Casp8_2^*$ generated by DISC [25, 26, 28], which is consistent with previous experiments.

4 Model reduction

In this section we use the PEA method to investigate the large apoptosis system (3.1). This system contains 13 reversible reactions: (H7), (H9), (H11), (H12), (H14), (H16), (H17), (H18), (H20), (H22), (H23), (H24) and (H25). In our preliminary work [23], we showed that the six reactions (H11), (H12), (H16), (H17), (H24) and (H25) are fast. Because the PEA method has a solid mathematical basis, it can be used as a tool to determine whether or not a reversible reaction is fast. After many attempts by assuming some of the rest 7 reactions to be fast too, we find that the nine reversible reactions (H7), (H9), (H11), (H12), (H16), (H17), (H18), (H24) and (H25) can be well regarded as fast.

Here we derive the corresponding simplified model under the assumption that the nine reversible reactions are fast. According to the framework in Section 2, we decompose the concentration vector U as

$$U = \begin{pmatrix} X \\ Y \\ Z \end{pmatrix}.$$

Here X stands for the products of the nine reactions, Y for the reactants and Z for the rest:

$$\begin{aligned} X &= ([Casp8_2^* : Casp3], [Casp8_2^* : Bid], [tBid : Bax], [tBid : Bax_2], \\ &\quad [Bcl_2 : Bax], [Bcl_2 : tBid], [Cyto.c^* : Apaf : ATP], \\ &\quad [Cyto.c^* : Apaf : ATP : Casp9], [Cyto.c^* : Apaf : ATP : Casp9_2])^T, \\ Y &= ([Casp8_2^*], [Bid], [tBid], [Bax], [Bcl_2], [Cyto.c^*], [Apaf], [Casp9], [Casp3])^T, \\ Z &= ([Cyto.c], [Casp9^*], [Casp9^* : Casp3], [Casp3^*], [Smac], [Smac]^*, [XIAP], \\ &\quad [Smac^* : XIAP], [Casp9 : XIAP], [Casp3^* : XIAP])^T. \end{aligned} \tag{4.1}$$

With this decomposition, the kinetic equations in (3.1) can be rewritten as

$$\begin{aligned} \frac{dX}{dt} &= \frac{1}{\varepsilon} \hat{Q}_1(X, Y) + Q_1(X, Y, Z) \\ \frac{dY}{dt} &= \frac{1}{\varepsilon} \hat{Q}_2(X, Y) + Q_2(X, Y, Z) . \\ \frac{dZ}{dt} &= Q_3(X, Y, Z). \end{aligned} \tag{4.2}$$

Here the small parameter ε characterizes the fastness of the reversible reactions as in Section 2,

$$\begin{aligned}\hat{Q}_1(X, Y) &= \varepsilon(v_7, v_9, v_{11} - v_{12}, v_{12}, v_{24}, v_{25}, v_{16} - v_{17}, v_{17} - v_{18}, v_{18})^T, \\ \hat{Q}_2(X, Y) &= \varepsilon(-v_7 - v_9, -v_9, -v_{11} - v_{25}, -v_{11} - v_{12} - v_{24}, -v_{24} - v_{25}, -v_{16}, -v_{16}, -v_{17} - v_{18}, -v_7)^T,\end{aligned}$$

stand for the change rates of concentration due to the rapid reactions, and

$$\begin{aligned}Q_1(X, Y, Z) &= (-v_8, -v_{10}, 0, 0, 0, 0, 0, v_{19}, -v_{19})^T, \\ Q_2(X, Y, Z) &= (v_8 + v_{10} + v_0, 0, v_{10}, 0, 0, v_{15}, 0, -v_{22}, -v_{20})^T, \\ Q_3(X, Y, Z) &= (-v_{15}, v_{19} - v_{20} + v_{21}, v_{20} - v_{21}, v_8 + v_{21} - v_{23}, -v_{13}, v_{13} - v_{14}, -v_{14} - v_{22} - v_{23}, v_{14}, v_{22}, v_{23})^T,\end{aligned}$$

are those for the other reactions. It is direct to check that

$$\hat{Q}_2(X, Y) + \Theta \hat{Q}_1(X, Y) \equiv 0 \quad (4.3)$$

with Θ the following constant 9x9-matrix

$$\Theta = \begin{pmatrix} 1 & 1 & 0 & 0 & 0 & 0 & 0 & 0 & 0 \\ 0 & 1 & 0 & 0 & 0 & 0 & 0 & 0 & 0 \\ 0 & 0 & 1 & 1 & 0 & 1 & 0 & 0 & 0 \\ 0 & 0 & 1 & 2 & 1 & 0 & 0 & 0 & 0 \\ 0 & 0 & 0 & 0 & 1 & 1 & 0 & 0 & 0 \\ 0 & 0 & 0 & 0 & 0 & 0 & 1 & 1 & 1 \\ 0 & 0 & 0 & 0 & 0 & 0 & 1 & 1 & 1 \\ 0 & 0 & 0 & 0 & 0 & 0 & 0 & 1 & 2 \\ 1 & 0 & 0 & 0 & 0 & 0 & 0 & 0 & 0 \end{pmatrix}.$$

Recall that

$$\begin{aligned}v_7 &= k_7[Casp8_2^*][Casp3] - k_{-7}[Casp8_2^* : Casp3], \\ v_9 &= k_9[Casp8_2^*][Bid] - k_{-9}[Casp8_2^* : Bid], \\ v_{11} &= k_{11}[tBid][Bax] - k_{-11}[tBid : Bax], \\ v_{12} &= k_{12}[tBid : Bax][Bax] - k_{-12}[tBid : Bax_2], \\ v_{16} &= k_{16}[Cyto.c^*][Apaaf][ATP] - k_{-16}[Cyto.c^* : Apaaf : ATP], \\ v_{17} &= k_{17}[Cyto.c^* : Apaaf : ATP][Caps9] - k_{-17}[Cyto.c^* : Apaaf : ATP : Casp9], \\ v_{18} &= k_{18}[Cyto.c^* : Apaaf : ATP : Casp9][Casp9] - k_{-18}[Cyto.c^* : Apaaf : ATP : Casp9_2], \\ v_{24} &= k_{24}[Bcl_2][Bax] - k_{-24}[Bcl_2 : Bax], \\ v_{25} &= k_{25}[Bcl_2][tBid] - k_{-25}[Bcl_2 : tBid].\end{aligned} \quad (4.4)$$

Then for any given $Y = ([Casp8_2^*], [Bid], [tBid], [Bax], [Bcl_2], [Cyto.c^*], [Apaaf], [Casp9], [Casp3])^T$ with

positive components, we use (4.3) to get

$$X = \left([Casp8_2^* : Casp3], [Casp8_2^* : Bid], [tBid : Bax], [tBid : Bax_2], [Bcl_2 : Bax], [Bcl_2 : tBid], [Cyto.c^* : Apa f : ATP], [Cyto.c^* : Apa f : ATP : Casp9], [Cyto.c^* : Apa f : ATP : Casp9_2] \right)^T$$

with positive components such that $v_7 = v_9 = v_{11} = v_{12} = v_{16} = v_{17} = v_{18} = v_{24} = v_{25} = 0$. Thus, the principle of detailed balance is verified.

After verifying the conditions for the PEA method to be reliable, we turn to write down the simplified model. In view of (4.3), we define $\tilde{Y} = Y + \Theta X$. Then the ODEs in (4.2) become

$$\begin{aligned} \frac{dX}{dt} &= \frac{1}{\varepsilon} \hat{Q}_1(X, Y) + Q_1(X, Y, Z), \\ \frac{d\tilde{Y}}{dt} &= Q_2(X, Y, Z) + \Theta Q_1(X, Y, Z), \\ \frac{dZ}{dt} &= Q_3(X, Y, Z). \end{aligned} \tag{4.5}$$

Guided by the framework in Section 2, we solve $\hat{Q}_1(X, Y) = 0$, namely,

$$\left\{ \begin{array}{l} v_7 = k_7[Casp8_2^*][Casp3] - k_{-7}[Casp8_2^* : Casp3] = 0, \\ v_9 = k_9[Casp8_2^*][Bid] - k_{-9}[Casp8_2^* : Bid] = 0, \\ v_{11} = k_{11}[tBid][Bax] - k_{-11}[tBid : Bax] = 0, \\ v_{12} = k_{12}[tBid : Bax][Bax] - k_{-12}[tBid : Bax_2] = 0, \\ v_{16} = k_{16}[Cyto.c^*][Apa f][ATP] - k_{-16}[Cyto.c^* : Apa f : ATP] = 0, \\ v_{17} = k_{17}[Cyto.c^* : Apa f : ATP][Casp9] - k_{-17}[Cyto.c^* : Apa f : ATP : Casp9] = 0, \\ v_{18} = k_{18}[Cyto.c^* : Apa f : ATP : Casp9][Casp9] - k_{-18}[Cyto.c^* : Apa f : ATP : Casp9_2] = 0, \\ v_{24} = k_{24}[Bcl_2][Bax] - k_{-24}[Bcl_2 : Bax] = 0, \\ v_{25} = k_{25}[Bcl_2][tBid] - k_{-25}[Bcl_2 : tBid] = 0. \end{array} \right.$$

From these algebraic equations we can easily solve X in terms of Y :

$$\begin{aligned}
[Casp8_2^* : Casp3] &= \frac{k_7[Casp8_2^*][Casp3]}{k_{-7}} = K_7[Casp8_2^*][Casp3], \\
[Casp8_2^* : Bid] &= \frac{k_9[Casp8_2^*][Bid]}{k_{-9}} = K_9[Casp8_2^*][Bid], \\
[tBid : Bax] &= \frac{k_{11}[tBid][Bax]}{k_{-11}} = K_{11}[tBid][Bax], \\
[tBid : Bax_2] &= \frac{k_{12}[tBid:Bax][Bax]}{k_{-12}} = K_{12}K_{11}[tBid][Bax][Bax], \\
[Cyto.c^* : Apaf : ATP] &= \frac{k_{16}[Cyto.c^*][Apaf][ATP]}{k_{-16}} = K_{16}[Cyto.c^*][Apaf][ATP], \\
[Cyto.c^* : Apaf : ATP : Casp9] &= \frac{k_{17}[Cyto.c^*:Apaf:ATP][Casp9]}{k_{-17}} \\
&= K_{17}K_{16}[Cyto.c^*][Apaf][ATP][Casp9], \\
[Cyto.c^* : Apaf : ATP : Casp9_2] &= \frac{k_{18}[Cyto.c^*:Apaf:ATP:Casp9][Casp9]}{k_{-18}} \\
&= K_{18}K_{17}K_{16}[Cyto.c^*][Apaf][ATP][Casp9]^2, \\
[Bcl_2 : Bax] &= \frac{k_{24}[Bcl_2][Bax]}{k_{-24}} = K_{24}[Bcl_2][Bax], \\
[Bcl_2 : tBid] &= \frac{k_{25}[Bcl_2][tBid]}{k_{-25}} = K_{25}[Bcl_2][tBid]
\end{aligned} \tag{4.6}$$

with $K_i = k_i/k_{-i}$ for $i = 7, 9, 11, 12, 16, 17, 18, 24, 25$. Denote these relations by $X = \Psi(Y)$.

It is remarkable that the relations rely only on the 9 constants K_i , instead of the 18 constants $k_{\pm i}$. The latter are often not reliably known.

Substituting $X = \Psi(Y)$ into the second and third equations in (4.5), we obtain

$$\begin{cases} \frac{d\tilde{Y}}{dt} = Q_2(\Psi(Y), Y, Z) + \Theta Q_1(\Psi(Y), Y, Z), \\ \frac{dZ}{dt} = Q_3(\Psi(Y), Y, Z) \end{cases}$$

and thereby gain equations for Y :

$$\frac{dY}{dt} = (I + \Theta\Psi(Y)_Y)^{-1} \frac{d\tilde{Y}}{dt} = (I + \Theta\Psi(Y)_Y)^{-1} (Q_2(\Psi(Y), Y, Z) + \Theta Q_1(\Psi(Y), Y, Z)).$$

Consequently, the original system (3.1) of 28 ODEs can be approximated by the following 19 ODEs

$$\begin{aligned}
\frac{dY}{dt} &= (I + \Theta\Psi(Y)_Y)^{-1} (Q_2(\Phi(Y), Y, Z) + \Theta Q_1(\Psi(Y), Y, Z)), \\
\frac{dZ}{dt} &= Q_3(\Psi(Y), Y, Z)
\end{aligned} \tag{4.7}$$

together with nine algebraic relations

$$X = \Psi(Y)$$

being detailed in (4.6). Recall that Y and Z are defined in (4.1). We call this new simplified model as ISS-2.

Table 3: The ISS skeleton model due to Okazaki et al. (2008)

Reaction	Rate constant
(S1) $Casp8_2^* + Casp3 \rightarrow Casp8_2^* + Casp3^*$	$6.25.00 \times 10^{-6} nM^{-1} s^{-1}$
(S2a) $Casp8_2^* + Bid \rightarrow Casp8_2^* + 0.0328tBid : Bax_2$	$vS2a = \frac{k_a [Casp8_2^*][Bid]}{[Casp8_2^*] + K_a} (k_a = 0.1s^{-1}, K_a = 20nM)$
(S2b) $Cyto.c + tBid : Bax_2 \rightarrow 0.867Cyto.c^* : Apaf : ATP + tBid : Bax_2$	$1 \times 10^{-3} nM^{-1} s^{-1}$
(S2c) $Cyto.c^* : Apaf : ATP + 2Casp9 \rightarrow Cyto.c^* : Apaf : ATP + Casp9 + Casp9^*$	$1.46 \times 10^{-6} nM^{-1} s^{-1}$
(S2d) $Casp9^* + Casp3 \rightarrow Casp9^* + Casp3^*$	$1.96 \times 10^{-5} nM^{-1} s^{-1}$

5 Numerical simulations

The purpose of this section is to show the reliability of our ISS-2 model by resorting to numerical simulations. Precisely, we compare the ISS-2 model (4.6)–(4.7) with the entire ISS model (3.1) and Okazaki et al.’s ISS skeleton model [19] in several aspects, including the accuracy, M-D transition behavior and sensitivity. For the reader’s convenience, the skeleton model is given in Table 3. The simulations were carried out with Matlab.

5.1 Accuracy of the ISS-2 model

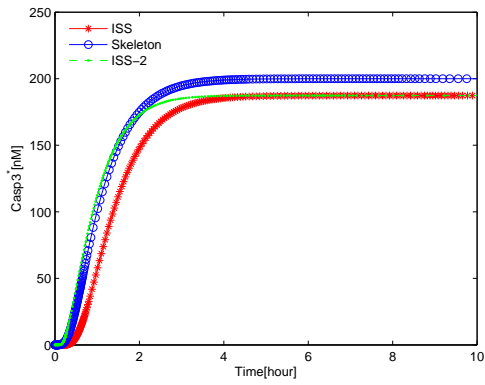
We compute the concentration of each species as functions of time t for the entire ISS model, the ISS skeleton model and our ISS-2 model, with initial concentrations from Table 2. Fig. 3(a) displays three curves of Casp3* as functions of time t corresponding to the three models. In this figure, the equilibrium value of Casp3*—the indicator of apoptosis—of the ISS-2 model is almost the same as that of the ISS model, whereas that of the skeleton model is slightly larger. The equilibrium values of all other species for the ISS model and our ISS-2 model are also very close to each other. The curves of Casp3, Casp9* and Bid as functions of time t are given in Fig. 3(b), Fig. 3(c), and Fig. 3(d), respectively. These numerical results show that our ISS-2 model is a reliable simplification of the entire ISS model.

5.2 M-D transition behavior

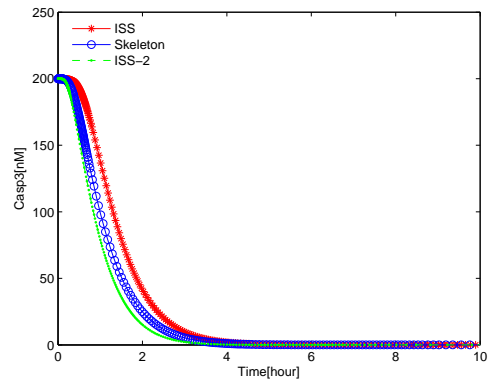
The M-D transition behavior is explained at the end of Section 3. In [19], it was reported that initial concentrations of Casp9 also have considerable impacts to the transition behavior. In order to study this behavior, Okazaki et al. introduced two quantities γ_D and v_0^C in [19]. The former was defined as the ratio of the net production of Casp3* via the D-channel to its total production, while the latter represents the critical value of v_0 (the generation rate for Casp8₂^{*}) corresponding to $\gamma_D = 0.5$. Note that, at $\gamma_D = 0.5$, the effect of the M-channel is same as that of the D-channel.

As previously, we use the initial concentrations from Table 2 and numerically solve the three models to obtain three curves of γ_D as a function of v_0 . The results are shown in Fig. 4(a). From this figure, we see that the curve given by the ISS-2 model matches that by the ISS model quite well and is obviously better than that by the skeleton model.

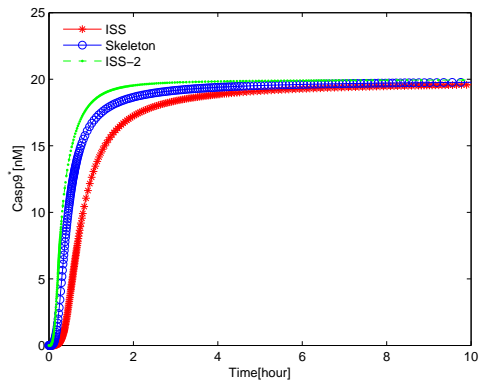
The curves of v_0^C as a function of the initial concentration of Casp9 are shown in Fig. 4(b). From this figure we see that when the initial concentrations of Casp9 are small, the values of v_0^C for the three models are almost the same. However, when the initial concentrations of Casp9 are large, the ISS skeleton model behaves quite different from the ISS model. But our ISS-2 model still matches the ISS model very



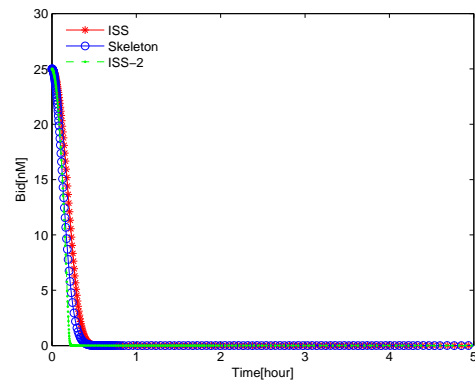
(a) The curves of Casp3* as functions of t



(b) The curves of Casp3 as functions of t



(c) The curves of Casp9* as functions of t



(d) The curves of Bid as functions of t

Figure 3: Comparison of the ISS model (red asterisk), the skeleton model (blue open circle) and our ISS-2 model (green dot). The initial concentrations are from Table 2. (a): the curves of Casp3* as functions of t . (b): the curves of Casp3 as functions of t . (c): the curves of Casp9* as functions of t . (d): the curves of Bid as functions of t .

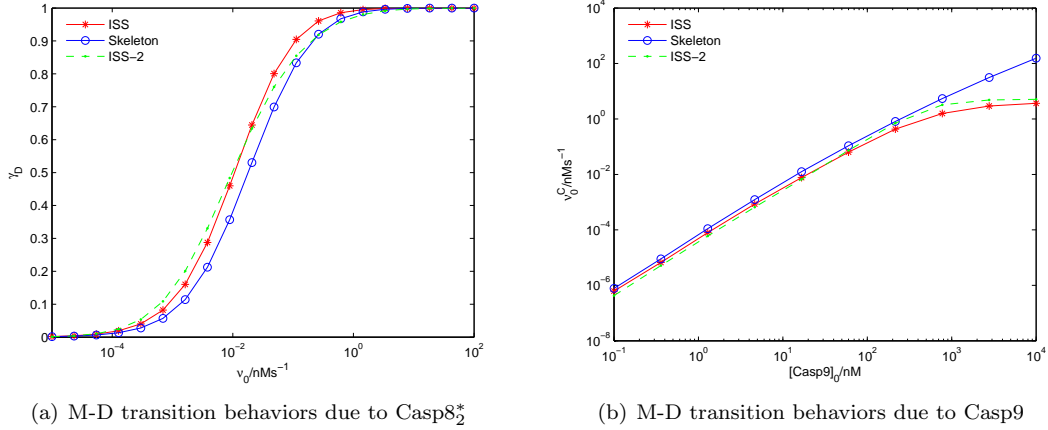


Figure 4: Comparison of the ISS model (red asterisk), the skeleton model (blue open circle) and the ISS-2 model (green dot) for the M-D transition behavior. (a): M-D transition behavior due to Casp8₂^{*}. (b): M-D transition behavior due to Casp9.

well. All these indicate that our ISS-2 model can well describe the actual M-D transition behavior and are much better than the ISS skeleton model.

5.3 Sensitivity Analysis

Now we present some results on the sensitivity of our ISS-2 model. Because the half-time—the time for Casp3^{*} to attain half of its equilibrium value—is an important quantity to characterize how fast a cell will die [6], we compute this quantity for the three models with initial data changed by one or two orders of magnitude higher and lower than the baseline values given in Table 2. The numerical results are shown in Fig. 5.

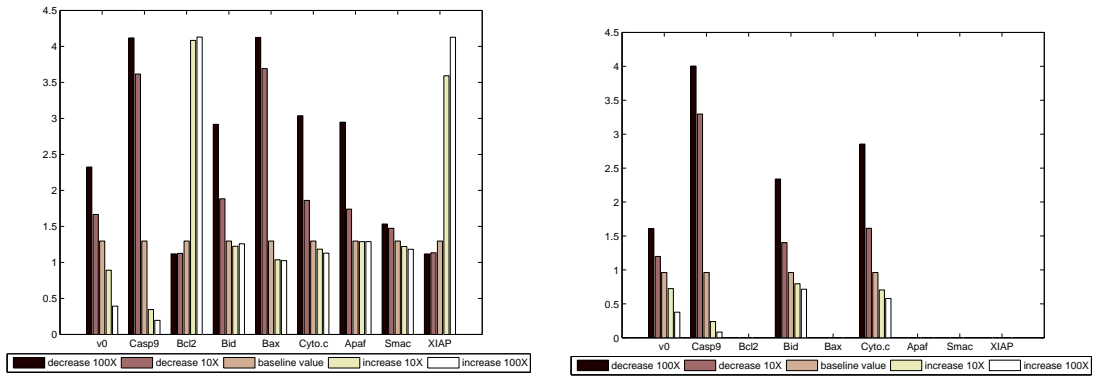
From Fig. 5 we see that, like the full apoptosis model due to Hua et al. [6], our ISS-2 model possesses the symmetrical or asymmetrical properties of varying each species to the outcome. The result by the ISS-2 model is very similar to that by the ISS model. A bit difference is that the half-time for the ISS-2 model is a little shorter than that for the ISS model, which is same as for the ISS skeleton model. This is expected because the assumption of fast reactions slightly speeds up the whole apoptotic process.

To evaluate our simplified model, we follow our previous work [23] and introduce the quantity

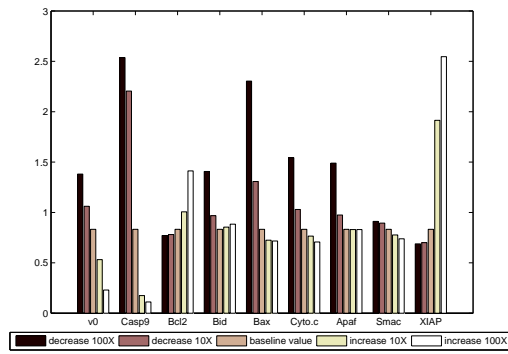
$$\alpha_{C3^*} = \frac{\text{equilibrium value of Casp3}^* \text{ for ISS-2}}{\text{equilibrium value of Casp3}^* \text{ for ISS}}$$

to examine how different are the equilibrium values of Casp3^{*} for the two models when changing initial concentrations of a certain species. When initial concentrations of some species are changed, α_{C3^*} will likely change too. For a good simplified model, such a quantity should be close to one.

We compute α_{C3^*} for changing initial concentrations of each species, including Casp3^{*}, by one or two orders of magnitude higher and lower than the baseline values as before. The result is given in Fig. 6. This result illustrates that α_{C3^*} is insensitive to most of initial concentration changes, except a little sensitivity for Bcl2 and Bax. In conclusion, our ISS-2 model well retains the main features of the ISS model and therefore can be viewed as a reliable simplification to the original ISS model.



(a) Half-time for activating Casp3 via the ISS model (b) Half-time for activating Casp3 via the skeleton model



(c) Half-time for activating Casp3 via the ISS-2 model

Figure 5: Sensitivity analysis of the ISS model, the skeleton model and the ISS-2 model. The overexpression or knockdown level of each species is changed one or two orders of magnitude of the baseline values while the others are unchanged.

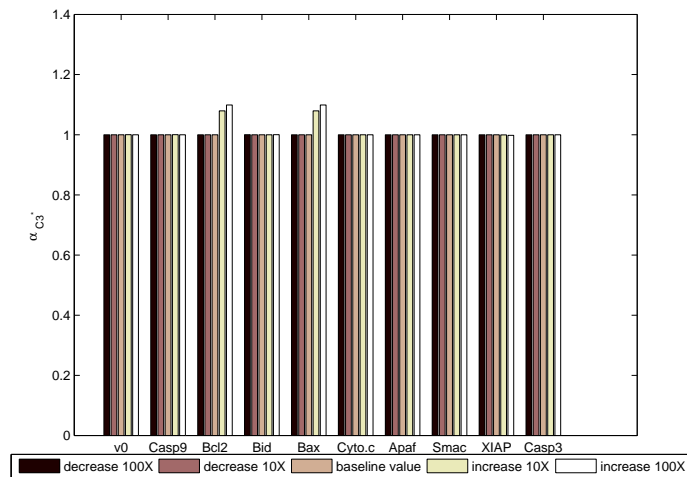


Figure 6: The change of α_{C3^*} against initial concentrations. The overexpression or knockdown level of each species is changed one or two orders of magnitude of the baseline values while the others are unchanged.

6 Summary

In this paper, we develop a general framework of the PEA method together with two conditions, under which the method can be justified rigorously. These conditions are the fastness assumption and the principle of detailed balance for fast reactions as a whole. Under these conditions, we simplify a general system of chemical reactions governed by the law of mass action. This simplification clearly has a solid mathematical basis.

Then we follow the general framework and study the ISS (intracellular–signaling subsystem) model as the downstream process of the Fas-signaling pathway model proposed by Hua et al. (2005) for human Jurkat T cells. Because the framework has a solid mathematical basis, it can be used as a tool to determine whether or not a reaction is relatively fast. After many attempts via numerical tests, we found that nine of reactions in the ISS model can be well regarded as fast.

Knowing that the nine reactions are faster than others, we use the justified PEA method and simplify the ISS model to derive a so-called ISS-2 model. It is remarkable that the reversible reactions in apoptosis obey the principle of detailed balance naturally. With numerical simulations, we compare the ISS-2 model with the ISS model as well as Okazaki’s ISS skeleton model in several aspects, including the accuracy, M-D transition behavior and sensitivity analysis. All the simulations show that the ISS-2 model is reliable. In particular, the new model can very well capture the M-D transition behavior of the ISS model at large initial concentrations of Casp9 and therefore improves Okazaki’s ISS skeleton model considerably (see Fig. 4(b)).

At present, we are trying to simplify the upstream process with the justified PEA method. In the future, we will also try to simplify the whole process by correctly combining the PEA method and the QSSA method.

Acknowledgments

This work was supported by the National Natural Science Foundation of China (NSFC 10971113) and by Specialized Research Fund for the Doctoral Program of Higher Education (Grant No. 20100002110085).

References

- [1] M. O. Hengartner, *The Biochemistry of apoptosis*, Nature 407 (2000), 770–776.
- [2] H. R. Horvitz, *Genetic Control of Programmed Cell Death in the Nematode Caenorhabditis elegans*, Cancer Res. 59 (1999), 1701–1706.
- [3] C. B. Thompson, *Apoptosis in the pathogenesis and treatment of disease*, Science 267(1995), 1456–1462.
- [4] M.E. Peter and P.H. Krammer, *The CD95(APO-1/Fas) DISC and beyond*, Cell Death Differ 10(2003), 26–35.

- [5] J. Keener and J. Sneyd, *Mathematical Physiology*, Springer, 1998.
- [6] F. Hua, M. G. Cornejo, M. H. Cardone, C. L. Stokes, and D. A. Lauffenburger, *Effects of Bcl-2 levels on Fas signaling-induced Caspase-3 activation: molecular genetic tests of computational model predictions*, J. Immunol. vol. 175(2005), 985–995.
- [7] S. W. Benson, *The Foundations of Chemical Kinetics*, McGraw-Hill, New York, 1960.
- [8] J. R. Bowen, A. Acrivos and A. K. Oppenheim, *Singular perturbation refinement to quasi-steady state approximation in chemical kinetics*, Chem. Eng. Sci. 18(1963), 177–188.
- [9] J. D. Ramshaw, *Partial chemical equilibrium in fluid dynamics*, Phys. Fluids 23(1980), 675–.
- [10] M. Rein, *The partial-equilibrium approximation in reacting flows*, Physics of Fluids A: Fluid Dynamics, 4(1992), 873–886.
- [11] D. A. Goussis and U. Maas, *Model Reduction for Combustion Chemistry*, Turbulent Combustion Modeling, 95 (2011), 193–220.
- [12] G. L. Schott, *Kinetic studies of hydroxyl radicals in shock waves. III. The OH concentration maximum in the hydrogen-oxygen reaction*, J. Chem. Phys. 32,710 (1960).
- [13] J. A. Miller and R. J. Kee., *Chemical nonequilibrium effects in hydrogen-air laminar jet diffusion flames*, J. Phys. Chem. 81, 2534 (1977).
- [14] S. B. Pope and S. M. Correa, *Joint pdf calculations of a non-equilibrium turbulent diffusion flame*, 21st Symposium (International) on Combustion (Combustion Institute, Pittsburgh, 1986), p. 1341.
- [15] N. Peters and F. Williams, *The asymptotic structure of stoichiometric methane-air flames*, Combust. Flame 68 (1987), 185–207.
- [16] N. Peters, *Multiscale combustion and turbulence*, Proc. Combust. Inst. 32(2009), 1–25.
- [17] N. Peters and B. Rogg, *Reduced Kinetic Mechanisms for Applications in Combustion Systems*, Springer-Verlag, Berlin, 1993.
- [18] M. D. Smooke,(ed.) *Reduced Kinetic Mechanisms and Asymptotic Approximations for Methane-Air Flames*, Lecture Notes in Physics 384, Springer, Berlin, 1991.
- [19] N. Okazaki, R. Asano, T. Kinoshita, and H. Chuman, *Simple computational models of type I/type II cells in Fas signaling-induced apoptosis*, J Theor. Biol. 250(2008), 621–633.
- [20] D. F. Walls, H. J. Carmichael, R. F. Gragg and W. C. Schieve *Detailed balance, Liapounov stability, and entropy in resonance fluorescence*, Phys. Rev. A 18(1978), 1622–1627.
- [21] W.-A. Yong, *An interesting class of partial differential equations*, J. Math. Phys. 49(2008), 033503–.
- [22] W.-A. Yong, *Singular perturbations of first-order hyperbolic systems with stiff source terms*, J. Differ. Eqns. 155(1999), 89–132.

- [23] Ya-Jing Huang and W.-A. Yong, *A Stable Simplification of a Fas-signaling Pathway Model for Apoptosis*, 2012 IEEE 6th International Conference on Systems Biology (ISB), 125–134.
- [24] A. Ashkenazi and V. M. Dixit, *Death receptors: signaling and modulation*, Science 281(1998), 1305–1308.
- [25] B. C. Barnhart, E. C. Alappat, and M. E. Peter, *The CD95 type I/type II model*, Semin. Immunol. 15(2003), 185–193.
- [26] A. K. Samraj, E. Keil, N. Ueffing, K. Schulze-Osthoff, and I. Schmitz, *Loss of caspase-9 provides genetic evidence for the type I/II concept of CD95-mediated apoptosis*, J. Biol. Chem. 281(2006), 29652–29659.
- [27] I. N. Lavrik, R. Eils, N. Fricker, C. Pforr, and P.H. Krammer, *Understanding apoptosis by systems biology approaches*, Mol. BioSyst. 5(2009), 1105–1111.
- [28] C. Scaffidi, S. Fulda, A. Srinivasan, C. Friesen, F. Li, K. J. Tomaselli, K. M. Debatin, P. H. Krammer, and M. E. Peter, *Two CD95 (APO-1/Fas) signaling pathways*, EMBO J. 17(1998), 1675–1687.